



Ciprofloxacin adsorption on a pomegranate peel adsorbent treated with oleic acid: Isotherm, kinetic, thermodynamic, and statistical studies

Hayder K. Admawi^{a,*}

a Department of Environmental Planning, Faculty of Physical Planning, University of Kufa, Al-Najaf, Iraq

Abstract

The performance of pomegranate peel treated with oleic acid (PPOA) was studied using a batch mode for ciprofloxacin (CIP) adsorption from an aqueous solution. Although other studies have investigated chemical modification with various chemical agents, the novel use of oleic acid for modification yields unprecedented results in terms of CIP removal efficiency. Dependent parameters were optimized using the sample pH, contact interval, initial CIP concentration, and adsorbent dose. Using response surface methodology (RSM) with a central composite design (CCD), a dose of 0.3 g/100 mL produced excellent removal efficiency (above 81%) for CIP concentrations of 60 mg/L after 90 minutes of contact at pH 6. With an R^2 (correlation coefficient) value of 0.985, analysis of variance (ANOVA) based on the CCD-RSM demonstrated a good fit between the experimental results and the predictions of the quadratic model. The Langmuir isotherm model was found to fit the CIP adsorption isotherms on the PPOA very well, with a theoretical maximum of 19.90 mg/g, indicating monolayer adsorption. Furthermore, a pseudo-second-order model could adequately describe the adsorption kinetics, implying that the adsorption rate is influenced by chemisorption. The main mechanisms underlying CIP biosorption are ion exchange and electrostatic attraction, whereas adsorption mechanics are controlled by external mass transfer and intra-particle diffusion. Thermodynamic analysis confirmed that adsorption was exothermic and spontaneous. After four consecutive repetitions, the adsorbent adsorption efficiency decreased from 81.88% to 50.91%, indicating its reusability. The results showed that pomegranate peel (PP) is an inexpensive adsorbent for CIP removal. Using this byproduct, CIP was effectively removed.

Keywords: Ciprofloxacin; Oleic acid; Adsorption; Pomegranate peels; Wastewater treatment.

Received on 21/02/2026, Received in Revised Form on 16/05/2026, Accepted on 17/05/2026, Published on 30/06/2026

<https://doi.org/10.31699/IJCPE.2026.2.8>

1- Introduction

Degradation of the environment and the depletion of natural resources have been linked to unchecked urbanization and industrialization [1]. Rapid industrial growth, urbanization, and the unsustainable use of natural resources all contribute to the release of large amounts of untreated wastewater into the environment, putting a strain on freshwater supplies [1, 2]. The majority of water contamination now comes from organic, inorganic, and microbiological pollutants, which pose significant public health and environmental risks [3]. Antibiotics are frequently used as antibacterial medications in both human and veterinary care [4]. Currently, contamination and increased bacterial resistance are caused by the widespread use of antibiotics and their release from human waste, veterinary fields, hospitals, and pharmaceutical companies [5, 6]. Two ways that antibiotics affect the environment are through the release of inappropriate wastewater and sewage or the disposal of expired medications [4]. However, the rapid increase in antibiotic production, of which over half are discharged into the environment, has led to several contamination issues [7]. Natural water sources and aquatic

environments have been shown to contain a variety of antibiotics. This indicates that traditional methods do not completely remove these contaminants from wastewater [8]. Antibiotic-resistant bacteria, a major public health concern, can be avoided by limiting antibiotic use and disposal to reduce their negative effects [9]. Recent research indicates that China is among the world's largest producers and consumers of antibiotics, with 162,000 tons of antibiotics produced and used annually [10, 11].

According to a European report published in 1996, more than 10200 tons of antibiotics were produced. In 2000, the United States produced more than 22700 tons of antibiotics [12]. By 2050, antimicrobial resistance is predicted to cause losses exceeding \$100 trillion and approximately 10 million deaths [13]. Ciprofloxacin (CIP) is the most widely used antibiotic worldwide due to its low cost and high effectiveness [14]. CIP is commonly used to treat animal and human diseases caused by bacteria, parasites, rickettsia, and fungi [15]. Some studies have indicated that the range of CIP concentrations in surface waters is from 2.5 to 6.5 mg/L [16]. Due to their hydrophilic properties and poor biodegradability, the



*Corresponding Author: Email: hayderk.abdulkareem@uokufa.edu.iq

© 2026 The Author(s). Published by College of Engineering, University of Baghdad.

This is an Open Access article licensed under a [Creative Commons Attribution 4.0 International License](https://creativecommons.org/licenses/by/4.0/). This permits users to copy, redistribute, remix, transmit and adapt the work provided the original work and source is appropriately cited.

proportion of antibiotics that can be digested in the bodies of animals and humans does not exceed 50% of the total antibiotic, and the rest is disposed of intact [15]. The presence of CIP in human drinking water can cause tremors, vomiting, headaches, nausea, and diarrhea [17]. These substances have the potential to cause cancer and harm living organisms. When present in wastewater treatment plants, they can lead to the formation of various byproducts during the ozonation or chlorination processes. Removal of CIP from wastewater is essential to prevent the development and spread of antibiotic-resistant bacteria [8]. CIP dissolves readily in water within a wide range of pH values and is very difficult for the environment to decompose [17]. To avoid these dangerous contaminants, treatment techniques should be thoroughly tested [4]. Electrocoagulation, ozonation, electro flotation, engineered wetlands, photocatalytic degradation, and Fenton degradation are all methods for extracting CIP from aqueous solutions [18]. Although the effectiveness of these techniques has been sufficiently proven, they still suffer several drawbacks, including high energy requirements, large quantities of sludge production, and complex operation [19, 20]. Adsorption is currently considered the most cost-effective, environmentally friendly, selective, and effective method of treating wastewater to remove antibiotics, dyes, and other organic pollutants [21]. It is one of the most important methods in lowering the pollution caused by pharmaceutically active compounds such as CIP in watery media [18].

Pomegranate peel is a popular natural biomass waste due to the large global production of pomegranate fruits. An estimated 1.5 million tons of Pomegranate peel (PP) are produced annually [22, 23]. Surprisingly, the peels and internal membrane comprise about half of the pomegranate fruit [24]. In addition to being readily available, pomegranate peels contain a number of natural functional groups that are important for pollutant adsorption and allow for the occurrence of several processes [25]. It is primarily made up of low relative molecular mass hydrocarbons such as cellulose, pectin, hemicellulose, lignin, and chlorophyll pigments. Therefore, researching agricultural byproducts and converting them into adsorbent materials is of paramount importance. PP is increasingly used as an environmentally friendly adsorbent for heavy metals, dyes, and some other pollutants. Many researchers have used a different activation process, whether base or acid, to increase the surface area and efficiency of the prepared surface, as well as the adsorption capacity of the adsorbents [26].

The PP is a great option for us because it is often available as bio-waste in many places and does not release any soluble contaminants into the treated water. Furthermore, because acid-treated PP may provide more active sites that can chemically interact with CIP, thus improving chemisorption, acid modification may enhance the adsorption of CIP ions. They can be used as effective adsorbents in both their natural and modified forms [24, 27]. Therefore, agricultural waste can be considered as a possible alternative to adsorbent materials [28]. Sareji et

al. [29] used high-quality activated carbon derived from pomegranate peels (PP) to extract several emerging pollutants from water and wastewater, including CIP, amoxicillin, diclofenac, and carbamazepine. Hassan and Ali [30] used black tea leaves and PP as adsorbent material to remove doxycycline from wastewater. They studied the adsorption behavior of PP and black tea leaves towards doxycycline using batch adsorption experiments, with controlled temperature, initial pH, adsorbent dosage, contact time, and initial contaminant concentration. According to their findings, the adsorption processes for PP and black tea leaves reached equilibrium after 90 and 150 minutes, respectively. Al-Badawi et al. [31] investigated the effectiveness of raw pomegranate peels as adsorbents for removing boron from aqueous solutions. The researchers found that treating modified pomegranate peel powder with both hydrochloric acid and sodium hydroxide increased removal efficiencies significantly. They also discovered that the adsorption capacity increases as the temperature and adsorbent doses increase. Rai et al. [32] used pomegranate peel modified with concentrated sulfuric acid as a bioadsorbent to extract hexavalent chromium from wastewater. Waghmare et al. [33] noted that the orthophosphoric acid-treated pomegranate peels had excellent removal efficiency and were able to remove more than 92% of methylene blue dye from aqueous solution. Instead of developing complex materials, this approach focuses on directly improving the natural pomegranate peel, which may provide a less expensive and simpler solution. This material, agricultural waste, was chosen because it offers significant advantages compared to other adsorbent materials, including cost-effectiveness, sustainability, increased efficiency, and an environmentally friendly method.

This study investigated the effectiveness of PP treated with oleic acid in extracting CIP from a contaminated aqueous solution, along with the adsorption mechanism, isotherm, kinetics, thermodynamics, and other aspects of the adsorption process. This study also used response surface methodology (RSM) to optimize the preparation conditions and assess the influence of variables such as initial CIP concentration, PPOA adsorbent, initial pH, and contact time on the PPOA adsorption capacity of CIP. To our knowledge, there hasn't been any investigation into the adsorption of CIP with pomegranate peel treated with oleic acid (PPOA) as an adsorbent and the subsequent regeneration of the PPOA. PPOA is therefore recommended as a novel adsorbent to extract CIP and TC from the aqueous environment.

2- Materials and methods

2.1. Materials

The Iraqi Samarra Pharmaceutical Company (Samarra, Iraq) supplied the antibiotic powdered ciprofloxacin (CIP) and tetracycline (TC). CIP has a chemical formula of $C_{17}H_{18}FN_3O_3$, purity of $\geq 98\%$, and molecular weight of 331 g/mol. TC has a molecular

weight of 480.9 g/mol, an assay of $\geq 98\%$, and a chemical formula of $C_{22}H_{25}ClN_2O_8$. Fig. 1A and Fig. 1B depict the chemical structure of CIP and TC. Sigma-Aldrich supplied oleic acid (assay $\geq 65\%$) and sodium chloride. Thomas-beaker supplied the sodium hydroxide (NaOH), acetone (99.9%), and hydrochloric acid (37%). All experiments used distilled water. All reagent-grade compounds were used without further purification.

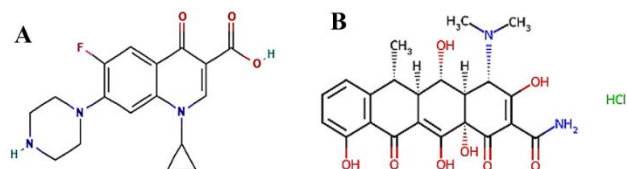


Fig. 1. Chemical structures of CIP, denoted as A, and TC, denoted as B.

2.2. Solution preparation

The batch adsorption experiment was conducted using synthetic wastewater. To prepare a stock CIP solution as model wastewater, a specific quantity of CIP was mixed with one liter of distilled water in the laboratory to make a synthetic solution of CIP (1000 mg/L). Before use, the synthetic CIP solution was vigorously stirred at 300 rotations/min for 20 minutes to ensure homogeneity. The stock solution was diluted to produce working solutions with the necessary concentrations. The solution's desired initial pH was adjusted using 0.1 M HCl and 0.1 M NaOH solutions.

2.3. Preparation of adsorbent material

The natural peels of pomegranates were gathered from juice vendors and Iraqi supermarkets, cut into small pieces, and then allowed to dry in the sun for two weeks. The peel's tough outer layer was repeatedly cleaned with tap water until the washing solution was clear, then rinsed with distilled water before baking for 24 hours at 100 degrees Celsius. After cooling to room temperature, it was thoroughly ground in a porcelain mortar and sieved to obtain particles no larger than 220 μm . To ensure a complete chemical reaction, 10 grams of pomegranate peel powder were ultrasonically dispersed in 250 mL of methanol in a 500 mL Erlenmeyer flask. The mixture was then stirred at 70°C for 4 hours with a magnetic stirrer at 300 rpm, with 100 mL of oleic acid added dropwise. After filtering the pomegranate peel residue, excess oleic acid is removed by washing it five times with acetone and deionized water. After cleaning, the pH of the solution was adjusted to the neutral range of 6.5 to 7.5. The saponification step is designed to improve the active sites of pomegranate peel and enhance the incorporation of CIP molecules onto its surface. The pomegranate peels are then collected and dried at 100°C for 12 hours before being left to cool. The resulting product, known as pomegranate peel treated with oleic acid (PPOA), was sieved to a size of 220 μm and stored in a sealed glass container for use in the experiment. To ensure the

accuracy of our findings, each experiment was repeated at least twice.

2.4. Experimental work

Response surface methodology (RSM) is a collection of mathematical and statistical methods for determining regression model equations and operating conditions based on quantitative data from relevant experiments. It can reduce the number of experiments needed to assess different parameters and their interactions [34]. In this work, the importance of four independent preparation variables (initial pH, PPOA adsorbent, contact time, and initial CIP concentration) and their interactions on the CIP removal by PPOA were investigated using a composite central experimental design (CCD). Table 1 shows that four independent variables (pH value, mixing time, PPOA dose, and initial CIP concentration) were changed at two different levels. To determine the optimum parameters for any type of adsorbent material, experiments were conducted on water samples contaminated with CIP at concentrations ranging from 30 to 90 mg/L. These samples were prepared from a stock solution of 1000 mg L^{-1} of CIP and initial pH values of 4 to 8. Using a pH meter (H260G, HACH, USA), (0.1 M) NaOH and (0.1 M) HCl were added to the original solution to adjust its pH. The adsorbent doses at room temperature ranged from 0.1 to 0.5 mg/L (refer to Table 1). In batch adsorption experiments, a specific amount of PPOA was mixed with 100 mL of CIP solution at a predefined starting concentration in 250 mL Erlenmeyer flasks. The flasks were kept at a steady solution temperature of $24 \pm 1^\circ\text{C}$ while being shaken at a speed of 200 rpm. To determine the most important factors influencing CIP removal by PPOA, a 2^3 factorial design (four independent parameters at two levels) was used with Design-Expert program version 13. This procedure enables the simultaneous analysis of multiple crucial parameters in a limited number of experiments [21, 22]. After the experiment, the samples were centrifuged at room temperature for 15 minutes at 4000 rpm. The upper solution of the sample was filtered using Whatman No. 4 filter paper (20-25 μm). Finally, the residual CIP content was determined using a UV-visible spectrophotometer (APEL PD-303 UV; Japan). The wavelength at which the absorbency measurement peaked was 276 nm. This measurement was taken after the solution reached a state of equilibrium. Each experiment was repeated twice, and the average of the results was recorded. After recovery, the percentage of CIP removal (R%) was determined using the following equation [35]:

$$R\% = \frac{CIP_0 - CIP_e}{CIP_0} \times 100 \quad (1)$$

The initial and final concentrations of the CIP in the sample are denoted by CIP_0 and CIP_e , respectively.

Eq. 2 was used to calculate the adsorption capacity.

$$q_e = \frac{CIP_0 - CIP_e}{M} \times V \quad (2)$$

where V and M stand for the solution volume in (L) and the PPOA weight in (gm), respectively, while q_e (mg/g) indicates the capacity of the adsorption.

Table 1. Parameter effects on PPOA adsorption

Symbol	Variables	Units	Factorial and center level		Axial level	
			-1	+1	$-\alpha$	$+\alpha$
A	PPOA dose	g/100 mL	0.1	0.5	0.1	0.5
B	Time	min	60	120	60	120
C	pH		4	8	4	8
D	CIP concentration	mg/L	30	90	30	90

3- Results and discussions

3.1. Determining the point of zero charge

The point of zero charge (pH_{PZC}) of the PPOA adsorbent was estimated using the pH drift methodology. This was achieved by creating a series of sodium chloride (NaCl) solutions with different pH values. The pH of the solutions was adjusted using trace amounts of HCl or NaOH to achieve the desired pH range of 2.0 to 12.0. Then, each solution of sodium chloride was mixed with the PPOA at room temperature, and the pH of each solution was measured after 24 hours. The pzc value was determined to be 4.55 by plotting the difference between the initial and final pHs versus the initial pH (see Fig. 2). This indicates the presence of a negative surface charge above pH 4.55 and a positive surface charge below pH 4.55. This data is useful for understanding the adsorption behavior, especially how pH affects the removal of CIP. In general, the adsorption of an anion on positively charged surfaces and a cation on negatively charged surfaces is easier [36]. The ciprofloxacin molecule exhibits a cationic and positive surface charge at pH values below 7, resulting from the protonation of its amine groups. The loss of a proton from the carboxylic group in the antibiotic's structure leads to the transformation of the ciprofloxacin molecule into an anionic form at pH values higher than 7 [37].

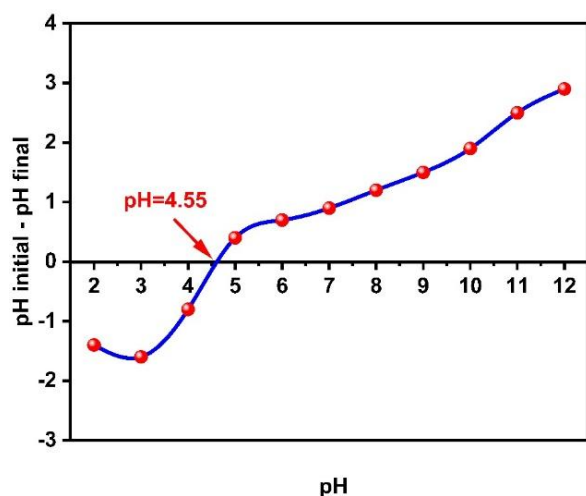


Fig. 2. Experimental point of the zero-charge (pzc) curve for PPOA

3.2. RSM optimization of CCD

The possible effects of independent parameters on CIP removal from the outfeed are displayed in Table 2. The predicted and experimental outcomes for CIP extraction efficiency are quite consistent. The test results showed that the highest CIP efficiency was 81.88% and the lowest was 48.73%. In accordance with RSM-CCD, the relationship between the independent variables and the CIP removal efficiency is represented in actual form by the following quadratic polynomial equation:

$$R\% = -31.61694 + 88.42875 * A + 0.345101 * B + 21.8745 * C + 0.807316 * D - 0.043958 * A * B + 1.76875 * A * C + 0.031667 * A * D - 0.004938 * B * C + 0.000154 * B * D + 0.009708 * C * D - 117.00278 * A^2 - 0.001474 * B^2 - 1.891278 * C^2 - 0.00908 * D^2 \quad (3)$$

The above equation, which expresses the reaction using actual factors, can be used to estimate specific quantities of the components. where R% denotes CIP's adsorption efficiency, and A, B, C, and D represent the PPOA dose (g/100 mL), mixing time (min), initial pH value, and CIP concentration (mg/L), respectively. The parameters AB, AC, AD, BC, BD, and CD interact with each other. A^2 , B^2 , C^2 , and D^2 indicate quadratic expressions for the process variables. Positive factor limits in equation (3) improve the efficiency of CIP removal, while negative factor limits reduce it.

Table 2. Experimental findings and responses

Run	Independent variables				Actual response	Predicted response
	A: PPOA dose	B: Time	C: pH	D: Concentration	R (%)	R (%)
1	0.5	60	4	90	55.37	54.78
2	0.3	90	8	60	70.9	70.27
3	0.1	60	8	90	48.73	48.55
4	0.5	120	8	90	53.21	52.20
5	0.1	60	4	90	52.04	50.23
6	0.1	60	8	30	59.58	60.11
7	0.1	120	4	90	54.4	54.40
8	0.3	90	6	30	79.76	78.12
9	0.5	60	8	90	50.02	50.27
10	0.1	120	4	30	66.98	67.73
11	0.1	120	8	90	51.36	51.54
12	0.3	90	6	60	81.88	80.26
13	0.5	120	8	30	59.63	62.44
14	0.3	90	6	60	80.92	80.26
15	0.3	120	6	60	81.767	80.32
16	0.1	60	4	30	64.37	64.12
17	0.5	90	6	60	77.09	76.69
18	0.5	120	4	90	57.42	57.89
19	0.1	120	8	30	63.21	62.54
20	0.5	120	4	30	71.55	70.47
21	0.3	90	4	60	73.44	75.12
22	0.3	90	6	60	81.14	80.26
23	0.3	60	6	60	75.05	77.55
24	0.1	90	6	60	73.02	74.47
25	0.5	60	4	30	67.08	67.90
26	0.3	90	6	90	63.36	66.05
27	0.5	60	8	30	62.33	61.06

3.3. Evaluation of the model

The variance of the independent parameters predicted by the correlation/model is represented by the R^2

(correlation coefficient) number; the closer the R^2 value is to 1, the more accurate the model [21]. Each parameter is significant and essential for evaluating the model of quadratic polynomials associated with the CIP removal process, as evidenced by the new model's R^2 value of 98.52%, which demonstrated a high degree of agreement between the predicted response model and the experimental results. This means that the model can account for 98.52% of the differences in the efficiency of the system. A high correlation between the predicted and actual values was indicated by the consistency of the R^2 of the adjusted and predicted values. The difference between the adjusted (96.80%) and predicted R^2 (91.69%) must be less than 0.20 to be considered appropriate. If not, there might be a problem with the data or the model. The actual vs. predicted plot confirms that the results obtained from the laboratory experiments are accurate and match the results that the model predicts because every point in Fig. 3 follows a straight line. These outcomes demonstrate that the operational variables and system can be employed to determine the CIP extraction from aqueous solution using the quadratic model.

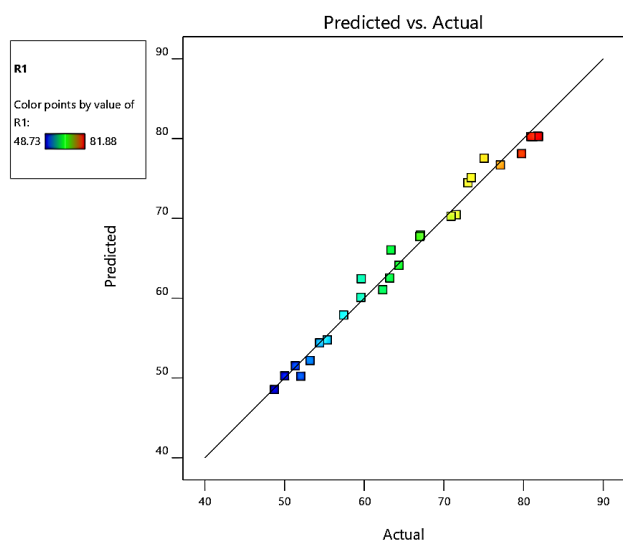


Fig. 3. Experimental and predicted CIP removal values

3.4. Analysis of the model

Each factor's statistical significance was determined using analysis of variance (ANOVA), and the results are shown in Table 3. P and F values are used to determine the significance of each factor on the removal efficiency; the smaller the P value and the higher the F value, the more significant the factor's impact on the efficiency of CIP removal [38]. The importance of the model was demonstrated by the F values for the CIP removal utilizing the PPOA, which were computed at 57.17. The likelihood of an F-value this high occurring as a result of noise is 0.01%. When the P-value is less than 5%, the model terms are considered highly accurate and significant with a confidence level greater than 95%. A regression analysis with a p-value less than 10^{-4} highlights the model's significance. Statistically significant model terms include A, B, C, D, A^2 , C^2 , D^2 ,

and C^2 . The signal-to-noise ratio is used to determine adequate accuracy, and it is best if this ratio exceeds four. The value of 21.93 in the current study indicates a suitable signal. The model is reproducible if the C.V. is less than 10%. The C.V. for CIP removal was less than 3%, indicating the reproducibility of the model [38]. Using the PPOA, the lack of fit value for CIP removal was found to be greater than 0.05 (P-value = 0.0546), indicating that the model is desirable and predictable.

Table 3. Results of the analysis of variance for the quadratic regression model for the CIP removal using PPOA adsorbents

Item	Sum of squares	Df	Mean square	F-number	p-number
Model	3021.84	14	215.85	57.17	<
A-Dose	22.24	1	22.24	5.89	0.0319
B-Time	34.60	1	34.60	9.17	0.0105
C-pH	106.00	1	106.00	28.07	0.0002
D-Concentration	654.98	1	654.98	173.48	<
AB	1.11	1	1.11	0.2948	0.5971
AC	8.01	1	8.01	2.12	0.1709
AD	0.5776	1	0.5776	0.1530	0.7026
BC	1.40	1	1.40	0.3719	0.5533
BD	0.3080	1	0.3080	0.0816	0.7800
CD	5.43	1	5.43	1.44	0.2536
A^2	56.32	1	56.32	14.92	0.0023
B^2	4.53	1	4.53	1.20	0.2951
C^2	147.17	1	147.17	38.98	<
D^2	171.85	1	171.85	45.52	<
Residual	45.31	12	3.78		0.0001
Lack of Fit	44.80	10	4.48	17.71	0.0546
Pure Error	0.5059	2	0.2529		
Cor Total	3067.14	26			
Std. Dev.	1.94				
C.V. %	2.95				
Mean	65.76				
Adeq. Precision	21.9366				
Predicted R^2	0.9169				
Adjusted R^2	0.9680				
R^2	0.9852				

3.5. Analysis and improvement

A typical probability versus residuals scheme can be used to assess the normality of a data set; if the curve appears almost linear, the information is assumed to follow a normal distribution [39, 21]. In Fig. 4A, the residual points on the normal probability diagram are aligned in a straight-line pattern, indicating sufficient and high reliability of the model. These results suggest that, given the model and operational variables used, the quadratic polynomial equation can be employed to evaluate CIP removal efficiency. Plotting the expected values against the residuals enables you to check the constant variance assumption. As shown in Fig. 4B, uneven error variances, outliers, and nonlinearity can be detected using the graph.

Furthermore, the random distribution of the internally studentized residuals between +4 and -4 did not reveal any outliers (Fig. 4C), indicating that the model fit was satisfactory.

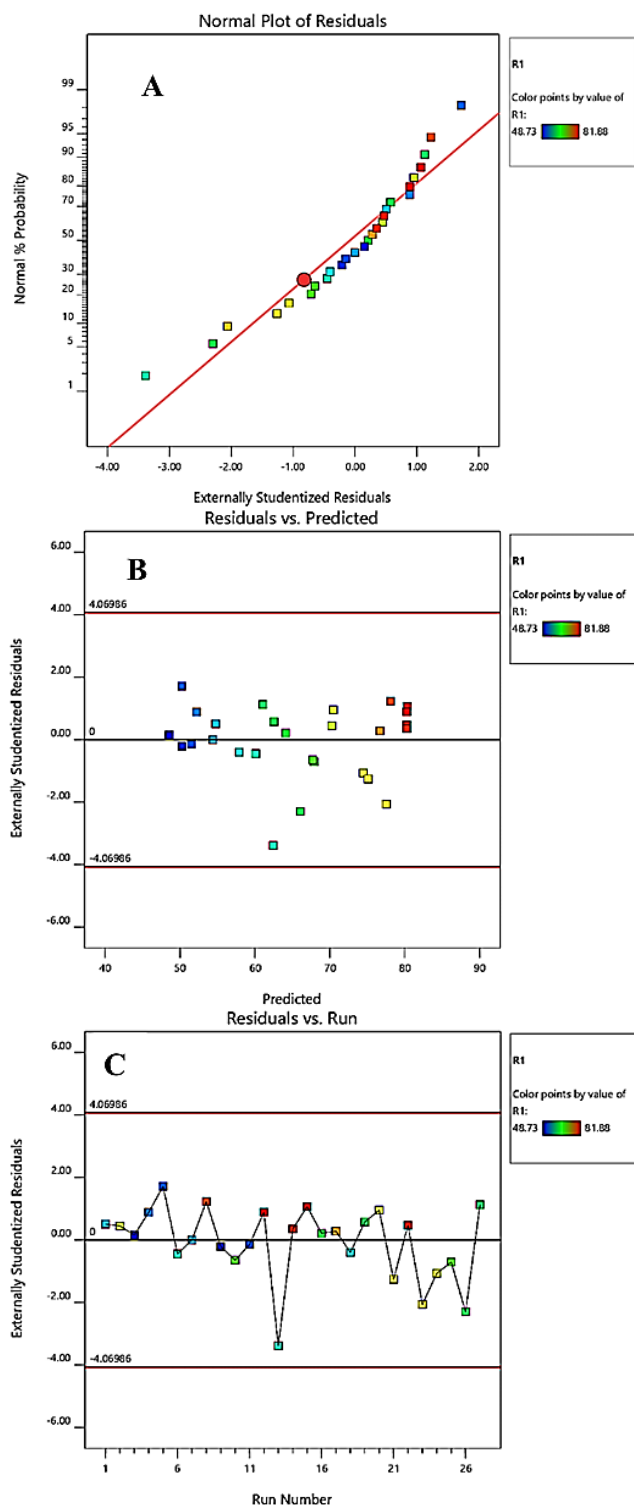


Fig. 4. (A) residuals plot of normal, (B) residual vs. predicted plot, and (C) the analysis of studentized run number vs. residuals

3.6. Validation and optimization of the CIP Removal Efficiency Procedure

The desired function analysis is one of the most widely used methods in applied science and engineering for optimizing various reaction processes [40]. Fig. 5 illustrates the optimal operating parameters that were

examined, namely the dose of PPOA, mixing time, initial pH, and CIP concentration. These four variables were expected to lead to a significant increase in the CIP extraction rate. Furthermore, under the suggested optimal operating parameters, the model was utilized to validate the experimental findings for the CIP removal efficiency percentage. Table 4 shows a 0.552% difference between the experimental removal values (77.92%) and the predicted removal value (78.35%) for adsorption. The modest percentage error thus demonstrated the significance and applicability of the generated RSM model.

Table 4. Predicted and experimental values for the percentage of CIP removal efficiency under optimal conditions

Dose (g/100 mL)	Time (min)	pH	CIP concentration (mg/L)	R (%) Pred.	R (%) Exp.	Error %
0.50	100	5.5	50 mg/L	78.35	77.92	0.552

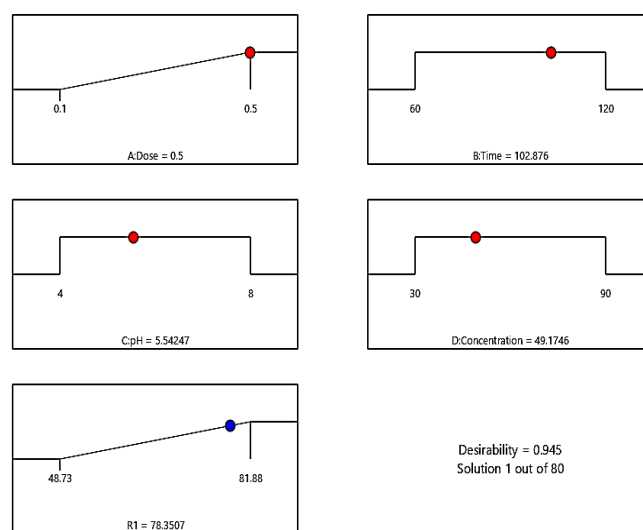


Fig. 5. Optimizing experimental variables depends on CIP extraction percentage (R%)

3.7. A model graph

Fig. 6 shows the main influence of four independent variables (dose, mixing time, pH, and CIP concentration) on the percentage of CIP removal. The model matched with 95% confidence intervals is represented by the black curves (dashed blue lines), whereas the red circles represent the design points that show experimental data. Each parameter's central points are most likely the location of optimal conditions where the greatest removal efficiency is recorded. A warning notice emphasizes that the independent variables interact in different ways, meaning that their effects are not entirely independent and are affected by synergistic relationships with other variables.

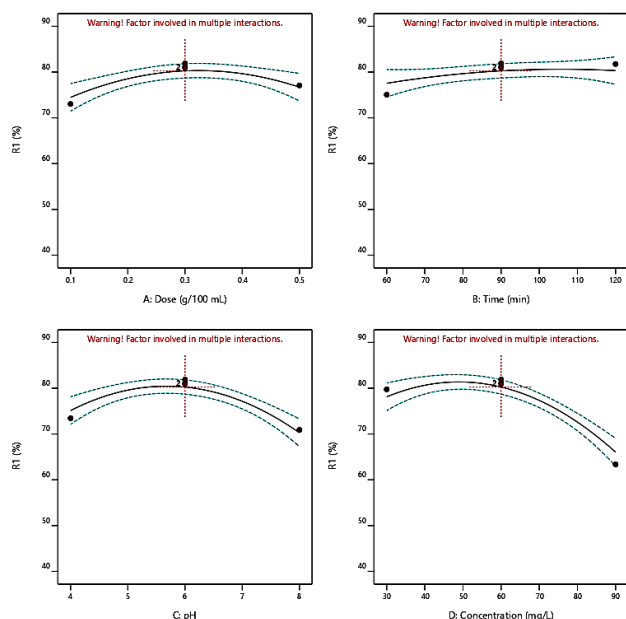


Fig. 6. Factors influencing CIP removal efficiency percentage, with response surfaces plotted to show parameter interaction

3.8. The effect of operational independent variables on the efficiency of CIP extraction

Contour graphs can be employed to evaluate the effect of parameters on CIP removal efficiency. The contour diagram of the relationship between the adsorbent PPOA dose and mixing time in relation to the extraction efficiency (CIP) are displayed in Fig. 7A. The contour lines in Fig. 7A show that raising the PPOA dosage along the dose axis from 0.1 to 0.3 g per 100 mL and the mixing time along the time axis from 60 to 120 minutes significantly increases efficiency. After that, the efficiency gradually decreases when the dosage reaches 0.5 g per 100 mL. Based on actual experimental findings, the highest CIP extraction efficiency (>81%) is achieved at an adsorbent dose of 0.3 g per 100 mL and a mixing time of 90 to 120 minutes in the plot center. The initially low removal efficiency is due to insufficient active sites to retain CIP molecules when using low doses of PPOA and short contact times. Removal efficiency is expected to increase with increasing dose of PPOA and mixing time until equilibrium is reached. Fig. 7B illustrates the contour diagram of the PPOA dose interaction with pH.

Fig. 7B has a well-defined area where the maximum extraction percentage is close to the 2D contour plot's center. The gradient of color, which runs from low efficiency (green color) to high efficiency (red color), indicates that using moderate to slightly low pH levels and adjusting adsorbent dosage enhances CIP removal. The contour lines (concentric contours) indicate a strong interaction between the two variables, with extraction efficiency increasing with both PPOA dose and initial pH value. The experimental conditions that were tested, represented by the red points (design dots), confirm the validity of the predicted response surface model. Removal efficiency drops at low pH levels (pH < 5) because CIP

molecules and hydrogen ions compete for the active sites of adsorption. However, the removal efficiency decreases at higher pH values (pH > 7), perhaps as a result of hydroxyl ions and CIP molecules competing for active adsorption sites. The effect of pH variations on the CIP molecule showed that the ciprofloxacin antibiotic's surface charge appears cationic and positively charged at pH values below 7 because of the protonation of its amine groups. The loss of a proton from the carboxylic group in the antibiotic's structure causes the CIP molecule to change into an anionic form at pH values higher than 7 [37]. Because its pH_{pzc} is 4.55, the PPOA is negatively charged at pH values above and below it. As a result, the removal efficiency is highest at pH 6. The explanation is that electrostatic attraction occurs when the oppositely charged entities reach their maximum at this range. When using a dose of approximately 0.3 g per 100 mL and pH 6, the highest CIP extraction rate is recorded, which approaches 81.88%.

The extraction rate of CIP is reduced at low doses because there are not enough adsorption sites to hold CIP molecules. On the other hand, excessive adsorbent dosage can cause particle agglomeration, which lowers the adsorption efficiency and available surface area. The impacts of PPOA dosage and initial CIP concentration on the extraction percentage of CIP are examined (Fig. 7C). The relationship between the concentration of CIP (C: mg per L) and PPOA dose (A: g per 100 mL) on extraction percentage (R% CIP) is shown by the contour distribution in Fig. 7C. This figure demonstrates that raising the CIP concentration from 30 to 60 mg/L and the adsorbent dose from 0.1 to 0.3 g per 100 mL increases efficiency. Maximum efficiency of CIP removal (81.88%) was noted at an initial CIP concentration of 60 mg/L and a PPOA dose of approximately 0.3 g/100 mL. As the concentration of CIP increases, extraction efficiency gradually decreases, confirming the need for higher PPOA doses to compensate for the reduced CIP extraction rate. Fig. 7D investigates the effect of time and pH on the removal efficiency of CIP. The contour diagram, which depicts the change in CIP extraction, is shown in Fig. 7D. Darker shades indicate higher values of CIP extraction. The model accuracy is confirmed by the points of the design, denoted by red circles, which match well with the contour lines. The optimal adsorption conditions have the highest removal efficiency (81.88%) at pH 6 and contact times ranging from 90 to 120 minutes. It appears that pH has a greater impact on CIP extraction rate because the lines of the contour are spaced closer along the initial pH values axis than along the time axis.

The efficiency of CIP extraction gradually improves with increasing pH value and mixing time, highlighting the importance of these variables in the adsorption process. The effects of mixing time and initial CIP concentration on CIP removal efficiency were studied (Fig. 7E). The contour distribution diagram (Fig. 7E) illustrates how the initial CIP concentration (D: mg/L) and contact time (B: min) interact to influence the CIP extraction rate. With the highest extraction rate (81.88%) concentrated in the central area when the initial CIP

concentration and mixing time are optimally combined, the color gradient changes from green to red, indicating an increase in CIP extraction rate. The contour lines form concentric oval shapes, indicating a distinct peak where efficiency increases when both factors are increased simultaneously. However, as the closely spaced lines flatten out, further increases in initial CIP concentration result in lower yields beyond a certain point.

The accuracy of the model was confirmed by the red points, which are design points that closely resemble the contour pattern. The low efficiency (~70%) in the lower left region, where both parameters are low, highlights the need for adequate initial pollutant concentration and mixing time for efficient adsorption. Fig. 7F shows the two-dimensional contour diagram of the relationship between initial CIP concentrations and pH value. The two-dimensional diagram (Fig. 7F) illustrates how pH value affects CIP removal efficiency, showing a marked improvement as pH rises from acidic to slightly acidic

conditions. The red area corresponds to CIP concentration levels of 30 to 60 mg/l and a pH range of 4.5 to 6.5, and this area has the highest efficiency rate (approaching 81.88%). Ciprofloxacin removal efficiency decreases at higher concentration levels of ciprofloxacin (over 60 mg/L), especially at pH values above 7. This is most likely due to hydroxyl groups reducing the PPOA material's adsorption capacity. On the other hand, the extraction efficiency increases as the pH approaches mildly acidic conditions (around pH 6), indicating that the active sites of the PPOA adsorbent become more easily accessible for interaction. This pattern illustrates that the initial CIP concentration has a greater impact on adsorption performance than the pH value. According to the observed trend, the best adsorption conditions are found in the slightly acidic to moderate pH range (4.5–6.5), where the PPOA has the greatest affinity for the CIP contaminant at concentrations between 30 and 60 mg/L.

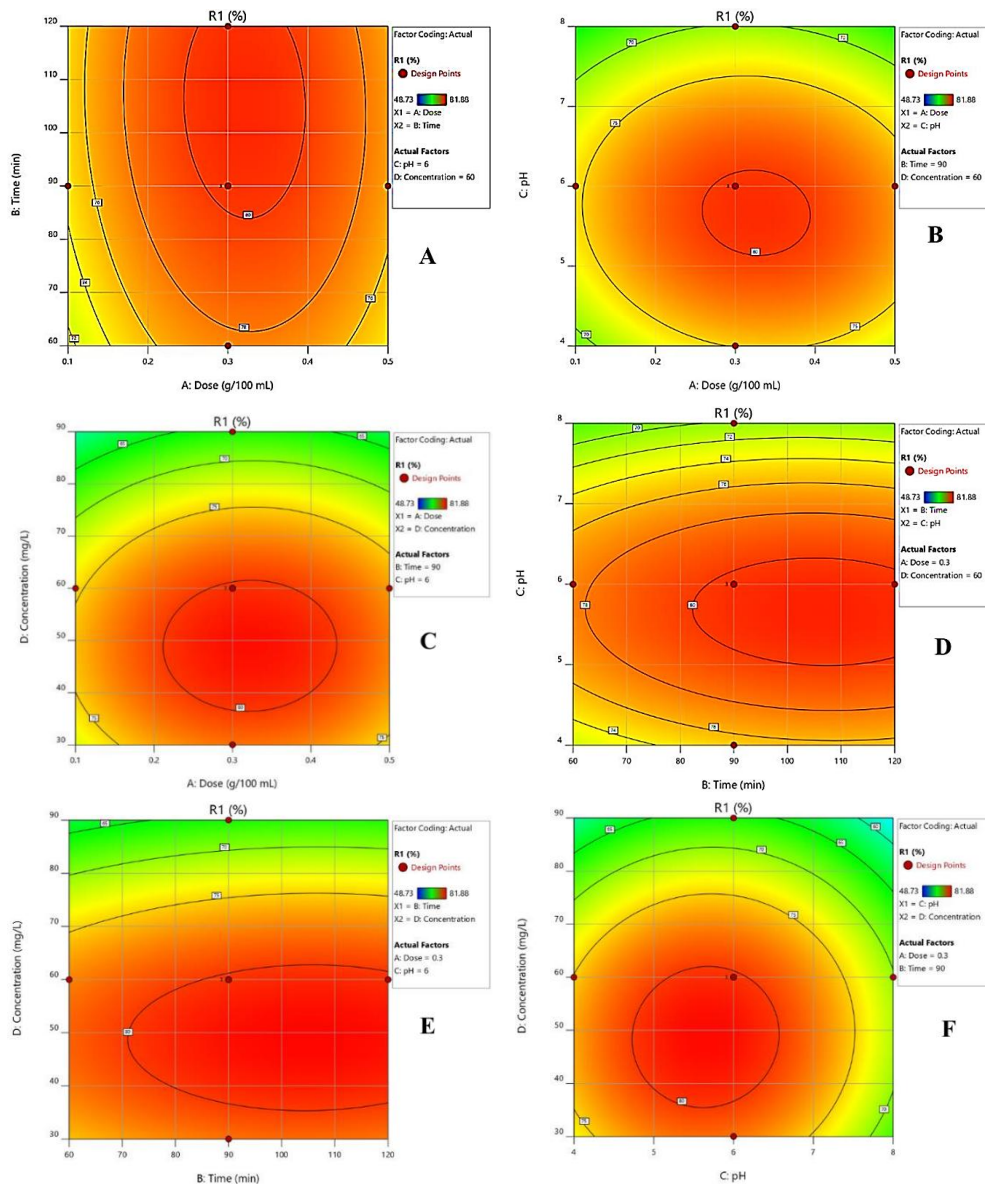


Fig. 7. Contour plot as a function of different parameters affecting the CIP removal

3.9. Examining models of isothermal adsorption

Adsorption is mathematically described by the isotherm model, which establishes a relationship between contaminant concentrations in the solid and liquid states at balance under particular thermal circumstances [41]. In this study, the Langmuir, Freundlich, and Temkin adsorption isotherms were constructed using CIP adsorption equilibrium data from the PPOA at initial adsorbate concentrations. The linear equations, isotherm values, and variables are compiled in Table 5. The Langmuir's model, with higher R^2 numbers, outperforms the Freundlich and Temkin models for CIP adsorption on PPOA (Fig. 8, Fig. 9, and Fig. 10, Table 5). But when compared to the Freundlich and Temkin models, the Langmuir model fits the CIP adsorption process better, suggesting that monolayer adsorption on PPOA dominated CIP adsorption. The classical Langmuir model assumes that there are no interactions between adsorbed species, the adsorption energy is constant throughout the surface, and all adsorbed species have equal access to homogeneous adsorption sites [42]. Assuming adsorption of a monolayer, the capacity of the Langmuir model was 19.90 mg per g. Depending on the Freundlich model parameters, even though the PPOA surface has some heterogeneity, the sites in the process still prefer uniform, monolayer adsorption, as demonstrated by the better fit of the Langmuir model.

Table 5. Parameters of isotherm models (Trial conditions: initial pH value was lowered to 6, temperature was $24 \pm 1^\circ\text{C}$, mixing speed was 200 rpm, and mixing time was 90 minutes)

Model name	Equation	Parameters	Values
Langmuir	$\frac{C_e}{q_e} = \frac{1}{q_{max}} K_1 + \frac{C_e}{q_{max}}$	K_1 (L/mg)	0.344
		q_{max} ($\text{mg} \cdot \text{g}^{-1}$)	19.90
		R^2	0.98
Freundlich	$\log q_e = \log K + \frac{1}{n} \cdot \log C_e$	K ((mg per g) (L per mg) $^{1/n}$)	5.662
		n	2.511
		R^2	0.95
		R^2	0.95
Temkin	$q_e = Bt \cdot \ln K_2 + Bt \cdot \ln C_e$	K_2 (L per mg)	5.727
		Bt	3.624
		R^2	0.95

Where: q_e (mg/g) denotes the amount of CIP adsorbed per unit mass of adsorbent particles in equilibrium, while the quantity of adsorbate needed to form a monolayer is known as q_{max} (mg/g). C_e (mg per L) is the liquid concentration of CIP at balance, and K_1 (L per mg) represents the equilibrium constant. n is the Freundlich constant that is related to the adsorption intensity. The isotherm constants for the Freundlich and Temkin isotherm models are denoted by K (mg/g (L/mg) $^{1/n}$) and K_2 (L/ mg), respectively. $Bt = RT/b$, where b is a constant related to the heat of adsorption, while R is the gas constant (8.31 J/mol K), and T (K) is the absolute temperature.

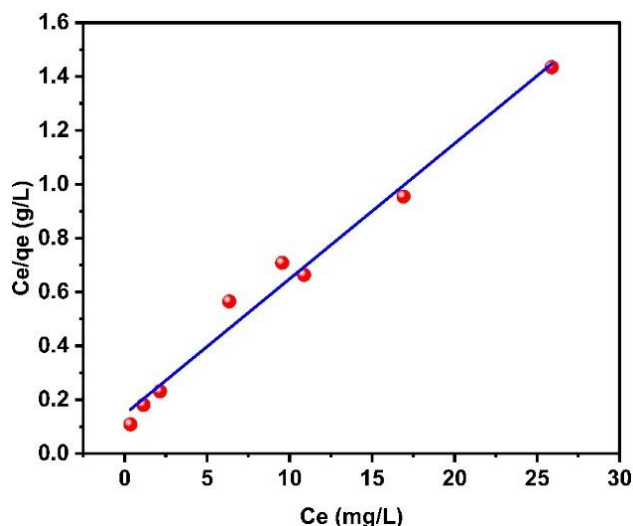


Fig. 8. Isotherm Langmuir model for CIP removal on PPOA surface

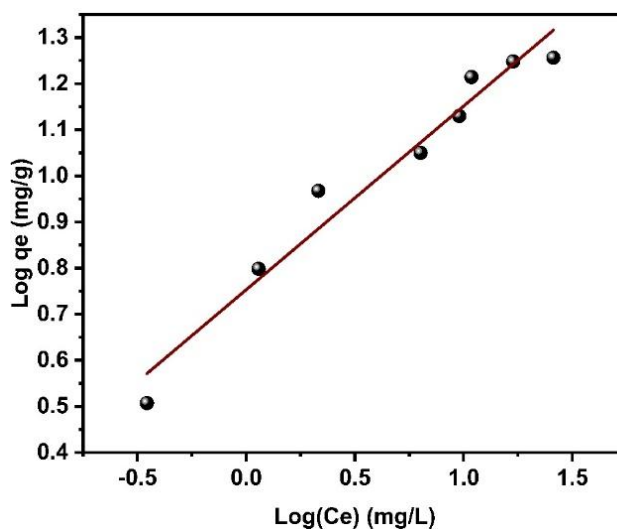


Fig. 9. Isotherm Freundlich model for CIP removal on PPOA surface

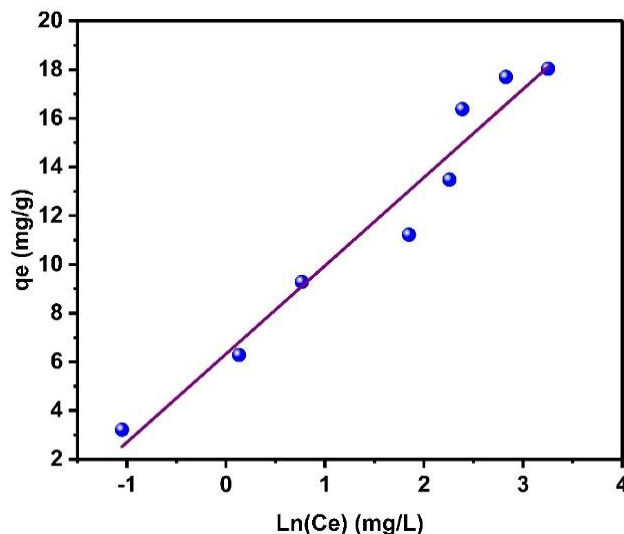


Fig. 10. Isotherm Temkin model for CIP removal on PPOA surface

3.10. Examining models of kinetic adsorption

The main factor influencing the design of an effective sorption process is the CIP transfer rate from the liquid phase to the solid phase [41]. The most widely used kinetic models-the pseudo first-order and pseudo second-order models-were employed to generate the kinetic data during the experimental work.

To calculate the adsorption rate of CIP extraction via the PPOA, these models have been selected. Table 6 lists linear equations and kinetic model characteristics. Fig. 11 and Fig. 12 show that the pseudo-second-order model accurately describes the adsorption process for CIP, with a correlation coefficient (R^2) of 0.98 and nearly identical calculated and experimental adsorption capacity. Under optimal conditions, the PPOA achieved an equilibrium capacity of 16.38 mg per g in 90 minutes.

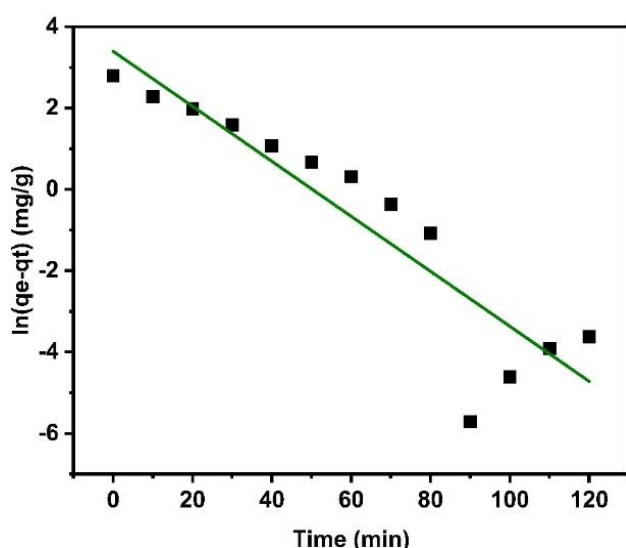


Fig. 11. CIP adsorption onto PPOA using a pseudo-first-order kinetic model

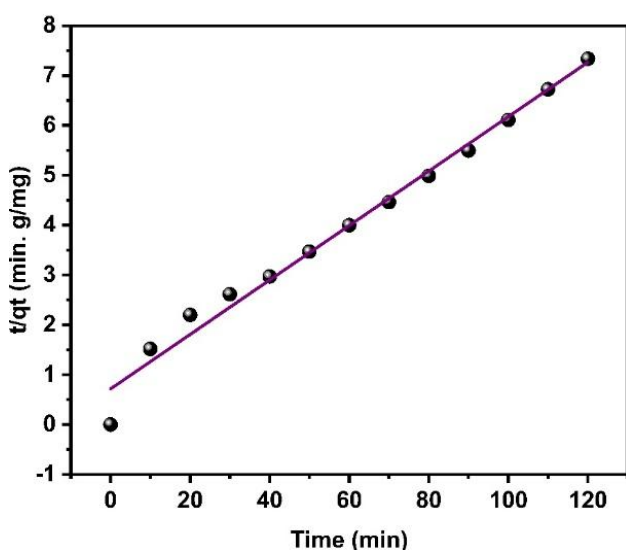


Fig. 12. CIP adsorption onto PPOA using a pseudo-second-order kinetic model

Table 6. Kinetic results for CIP uptake (experimental conditions: pH 6, temperature of 297 K, PPOA dose of 3 g/L, and CIP concentration of 60 mg/L)

Kinetic models	Equation	Parameters	Values
Pseudo-first order	$\ln(q_e - q_t) = \ln(q_e) - k_3 t$	q_e, exp	16.38
		q_e, cal	29.88
		k_3	0.0014
		R^2	0.83
Pseudo-second order	$\frac{t}{q_t} = \frac{1}{k_4 q_e^2} + \frac{1}{q_e} t$	q_e, exp	16.38
		q_e, cal	18.31
		k_4	0.0042
		R^2	0.98

Where: q_e (mg/g) and q_t (mg/g) are the amounts of CIP adsorbed at equilibrium and time t (min), respectively. k_3 (min^{-1}) is the rate constant in the pseudo-first-order model. k_4 (g/mg min) represents the pseudo-second-order equilibrium rate constant.

3.11. Thermodynamic studies

The thermodynamic parameters for the removal of CIP onto PPOA, namely the free energy (ΔG), entropy change (ΔS), and enthalpy change (ΔH), can be used to identify the type of adsorption. The additional batch experiment parameters (pH 6, dose 0.3 mg/L, initial CIP concentration 60 mg/L, and contact time 90 min) were fixed at an optimum level. Fig. 13 A. illustrates the impact of solution temperature on the adsorption behavior of CIP toward PPOA over a range of 24–44°C. Reduced CIP adsorption onto the PPOA surface was found when the solution temperature was raised (Fig. 13 A). As the temperature was increased from 24 to 44 °C, the removal efficiency decreased from 81.88% to 75.02% because solute mobility increased from the solid to the bulk phase. This results from heat release between the CIP and the active sites on the sorbent surface, as well as a decrease in physical adsorptive forces (van der Waals). The adsorption thermodynamic parameters can be calculated using the following formulas:

$$\Delta G = -RT \ln KL, KL = \frac{q_e}{C_e} \quad (4)$$

$$\Delta G = \Delta H - T\Delta S \quad (5)$$

Substituting Eq. 4 into Eq. 5 yields the Van't Hoff equation.

$$\ln KL = -\frac{\Delta H}{RT} + \frac{\Delta S}{R} \quad (6)$$

Enthalpy change (ΔH) and entropy change (ΔS) are calculated from the slope and intercept of a linear plot of $\ln(KL)$ against $1/T$ (Fig. 13B), where KL (dimensionless) is the balance thermodynamic constant. Table 7 lists the thermodynamic functions of the removal process. Spontaneous CIP adsorption onto the PPOA is indicated by the negative values of ΔG at all examined temperatures. Negative ΔH values indicate an exothermic

adsorption process. Furthermore, a decrease in degrees of freedom following CIP adsorption is indicated by the negative ΔS value.

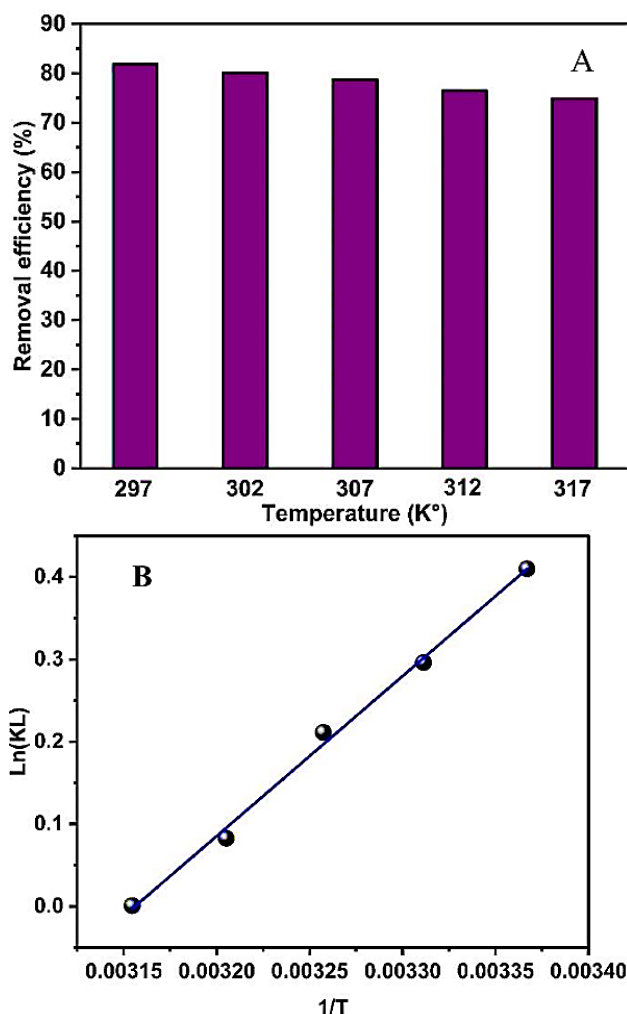


Fig. 13. (A) The influence of temperature on CIP adsorption; (B) Van't Hoff plot (dose 0.3 g/100 ml, pH 6, contact time 90 min, and CIP concentration 60 mg/L)

Table 7. Thermodynamic values of CIP adsorption on PPOA at various temperatures

Adsorbent	T (K)	KL	$\Delta G(\frac{KJ}{mol})$	$\Delta H(\frac{KJ}{mol})$	$\Delta S(\frac{J}{mol.K})$	R ²
PPOA	297	1.507	-1.012	-16.148	-50.962	0.995
	302	1.345	-0.743			
	307	1.235	-0.539			
	312	1.086	-0.214			

3.12. CIP adsorption mechanism into PPOA and intraparticle diffusion equation

The movement of the CIP from the aqueous solution to the PPOA can be explained by three primary mechanisms (three phases). When PPOA is added to the solution, CIP particles are first transferred. This process is not taken into account when creating kinetic systems because it is too fast [21]. The first phase, referred to as film diffusion, is the gradual transfer of CIP from the boundary layer to the surface of the PPOA adsorbent. The second phase occurs when the CIP reaches the PPOA surface and then

travels to the pores. The final phase incorporates the CIP's rapid adsorptive adhesion to active sites of the pore, which is fast and boring during kinetics engineering design [43, 44]. To assess the mechanism that controls kinetic reactions and to check whether diffusion is the rate-limiting step, and since the pseudo-first- and second-order models cannot determine how diffusion works, the kinetic model results were analyzed using an intraparticle diffusion model, which is expressed as follows [21, 45]:

$$qt = K_5 t^{0.5} + C \quad (7)$$

In this case, K_5 is calculated from the slope of the linear plots of qt vs. $t^{0.5}$, and C (mg/g) is the intercept, and K_5 is the intraparticle diffusion rate constant ($\text{mg}/\text{g} \cdot \text{min}^{0.5}$). The C values, R^2 (correlation constant), and K_5 are shown in Fig. 14. A linear diagram shows that the diffusion mechanism within the particles has a major impact on the kinetic sorption process. The spread indicates that the adsorption process takes place in three stages, demonstrating the graph's multi-linearity.

As shown in Fig. 14, the first phase of the adsorption process represents the film spread; the second phase represents the stepwise reaction of the adsorption, where the diffusion rate into particles or pores is the limiting step in the adsorption, while the third phase represents the stage of the equilibrium. A higher CIP molecule transfer rate within the PPOA surface K_5 ($3.114 \text{ mg/g} \cdot \text{min}^{0.5}$) is shown by the variables of the first trend line, and the negative value ($C=-0.002$) indicates that the adsorption rate was not affected by a boundary layer. However, a lower PPOA molecule transfer rate within the sorbent's pores is indicated by the second line's slightly lower value, K_5 ($1.489 \text{ mg/g} \cdot \text{min}^{0.5}$). The higher intercept value ($C = 11.007$) indicates an increased impact of the boundary on the adsorption rate. A high boundary influence on the adsorption rate is represented by the high C value (24.798) of the third line, whereas a slower transfer rate of the CIP molecules in the sorbent's pores is indicated by the negative low k value ($0.025 \text{ mg} \cdot \text{g}^{-1} \cdot \text{min}^{0.5}$).

An exothermic, spontaneous process was confirmed by the thermodynamic functions ($\Delta G^\circ < 0$, $\Delta H^\circ < 0$). The Langmuir ($R^2 = 0.98$) model and Freundlich ($R^2 = 0.95$) model demonstrate excellent fit, indicating monolayer surface of the adsorption on homogeneous active sites with some heterogeneity surface. The kinetic results support a mechanism of the multistep including fast adsorption on PPOA surface and then slower diffusion processes (the pseudo-second-order model). The pseudo-first-order model is preferred when high CIP concentration; however, the pseudo-second-order model best describes the adsorption process when the CIP concentration is low. This is because when the $\ln(q_e - q_t)$ value increases, function of error also rises, while when it falls, the error function decreases. Electrostatic attraction is another essential step in the adsorption process. Positively charged sites will probably be produced on the PPOA surface by adding oleic acid. CIP frequently exists as a zwitterion or anionic form

(negative charge), depending on the pH. These cationic surfaces (positively charged areas) on the modified PPOA attract the CIP anions when the CIP is negatively charged, allowing for efficient adsorption. At a slightly acidic pH, where many adsorption processes occur, this electrostatic attraction is especially advantageous [10, 46, 47]. Together, these various mechanisms demonstrate the efficacy and imply that this PPOA may be widely successful in eliminating CIP (and potentially other contaminants) in wastewater treatment.

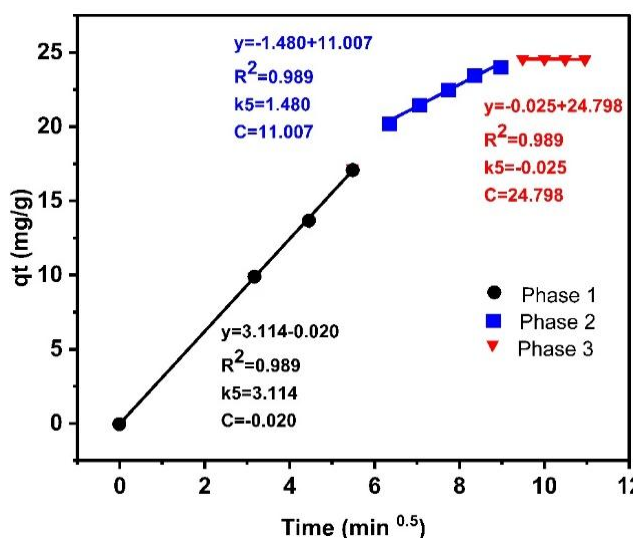


Fig. 14. Intra-particle diffusion diagram for CIP extraction by PPOA (trial conditions: pH 6, temperature of 297 K, PPOA dose of 3 g/L, and CIP initial concentration of 60 mg/L)

3.13. The study of regeneration

The reusable nature of the PPOA material is essential for its practical application in the CIP extraction from contaminated aqueous solutions. In the present work, a desorption process using a mild alkaline solution was used to regenerate CIP-loaded PPOA. After each adsorption cycle, the PPOA was treated with a 0.1 mol/L sodium hydroxide solution, thoroughly cleaned with distilled water, and oven dried. This procedure reduced material degradation while efficiently removing a significant portion of the CIP extraction, resulting in the regenerated PPOA for future applications. CIP molecules are bound together through strong electrostatic interactions during the adsorption process, which are essentially reversed. Fig. 15 depicts the sample's regeneration efficiency for four cycles. A gradual reduction in adsorption capacity was observed as a result of insufficient recovery of active sites post-regeneration, while the fourth cycle clearly caused a decrease in CIP adsorption, which could be attributed to adsorbed substance saturation. These findings demonstrate the PPOA's potent regeneration capacity. The material is an economical and sustainable adsorbent for CIP removal in wastewater treatment applications because it can be reused with minimal performance loss. Compared to

single-use adsorbents, its comparatively steady performance over a number of cycles indicates its potential for long-term use in continuous processing systems, which will drastically lower resource consumption and operating expenses [10, 48, 49].

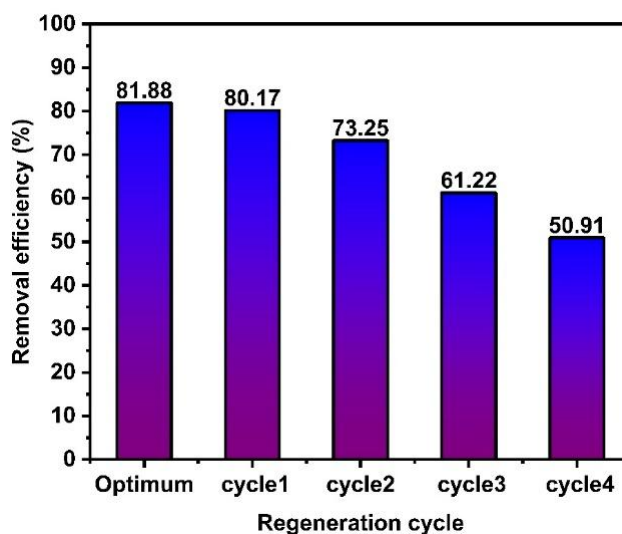


Fig. 15. Study of regeneration up to four cycles

3.14. Adsorption with selectivity

Tetracycline (TC) and ciprofloxacin (CIP) were combined to mimic real wastewater, which can contain a variety of antibiotics. The binary aqueous solutions were prepared using 30 mg per L of CIP and 30 mg per L of TC, while the single aqueous solution used 30 mg per L of CIP. To assess PPOA's ability to remove CIP and TC, under perfect circumstances, the adsorption process was completed (pH: 6, temperature: $24 \pm 1^\circ\text{C}$, mixing time: 90 min, PPOA dose: 3 g per L, mixing speed: 200 rpm, and CIP and TC concentration: 60 mg per L). The removal rate of CIP and TC by PPOA in a single antibiotic solution was 88.53% and 71.91%, respectively, as illustrated in Fig. 16. The CIP dye extraction rate in the mixed system stayed high at 80.04%.

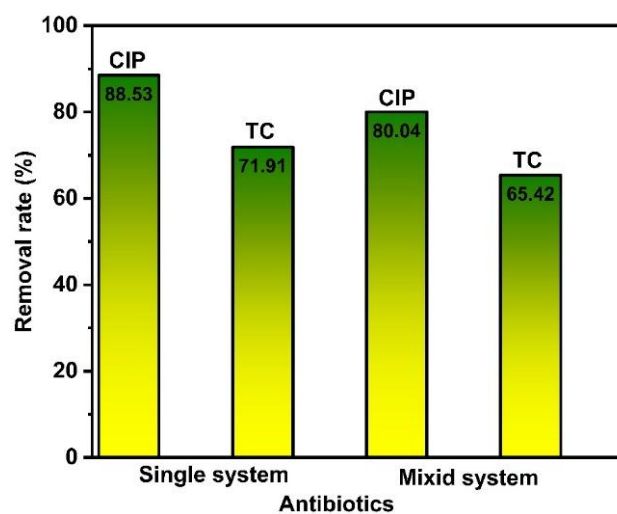


Fig. 16. PPOA selective adsorption

3.15. Comparing this adsorbent to others

The adsorption capacity of PPOA for CIP removal is contrasted with that of the other adsorbents reported in the literature in Table 8. The pomegranate peel treated with oleic acid had an adsorption capacity of 19.90 mg/g. This study demonstrated a relatively high adsorption capacity when compared to previous studies that used different adsorbents. The relatively high adsorption capacity of PPOA can be attributed to the modification by oleic acid and its effect on the surface properties of the PP. The addition of oleic acid to the PPOA modification may have increased the number of active sites or surface area, thus improving the adsorption process and increasing the attraction towards CIP. Furthermore, the addition of oleic acid may have altered the surface charge of the PP, increasing its ability to absorb ciprofloxacin. The modification may have enhanced the ability of the PPOA surface to interact with CIP by introducing various functional groups.

Table 8. Adsorption capacity comparison for CIP sorption using various adsorbents

Adsorbent	Adsorption capacity (mg/g)	References
Alginate bearing Mg–Al layered double hydroxide	38.46	[50]
Aloe vera based adsorbent	9.98	[12]
Pure fullerene (F)	23.5	[6]
ZnO nanoparticles	8.70	[51]
Groundnut shell powder	8.07	[51]
Oleic acid- pomegranate peel	19.90	The current study

3.16. The strength of this investigation

High adsorptive capacity: Oleic acid modification often increases PP's surface area and active sites, which enhances CIP removal efficiency. **Cost-effectiveness:** Because PP is an inexpensive and abundant natural material, it is an excellent adsorbent for large-scale wastewater treatment. **Environmental compatibility:** Using PP is compatible with eco-friendly treatment techniques and lowers secondary pollution. **Better surface characteristics:** Acid treatment increases porosity and adds functional groups, which can improve kinetics and adsorption capacity.

3.17. Practical restrictions

Although PPOA shows excellent performance in CIP uptake, there are some problems that need to be solved for practical application in subsequent studies. Firstly, developing a wide range of cost-effective industrial production techniques remains a challenge, as the preparation method used in this research is based on laboratory-level procedures. Second, although its performance in simulated aqueous solutions has been validated, the material's selectivity and long-term performance in more complex wastewater (real wastewater), which contains a wider range of contaminants, pH variations, and other factors, still need to be assessed. Finally, further research is needed to

ensure the feasibility of using PPOA in fixed-bed systems at the industrial level, given its stability over time and mechanical strength. These shortcomings highlighted the need for further research in the field of biosorbents to develop more stable, less expensive, and interference-resistant biosorbents.

4- Conclusions

Pomegranate peels, which are a solid agricultural waste, were used as adsorbent materials. The results of this study showed that PPOA can effectively extract CIP from contaminated aqueous solutions. The adsorption rate of CIP increases with the amount of PPOA adsorbent material due to the increased contact area, and the adsorption rate decreases at high initial concentrations of CIP. The maximum adsorption capacity was 19.90 mg/g when 0.3 g of PPOA was used to remove CIP from an aqueous solution (100 mL) containing 60 mg/L of CIP at pH 6 and a mixing time of 90 minutes. Under these optimal conditions, the maximum adsorption efficiency of CIP was over 81%. This was achieved by optimizing the process using Central Composite Design (CCD) within Response Surface Methodology (RSM). Using the RSM methodology, a second-order polynomial equation was derived to express the relationship between adsorption efficiency on PPOA-adsorbent materials and the effective parameters.

The results show that the initial CIP concentration, initial pH, contact time, and adsorbent dosage all have a significant impact on CIP adsorption efficiency. In addition, the PPOA adsorbent retains approximately 51% of its capacity after four reuse cycles, demonstrating its high reusability. In contrast, three well-known models, Langmuir, Freundlich, and Temkin were used to evaluate the experimental results obtained in this study. The obtained coefficient values show that the Langmuir model is more appropriate than the Freundlich and Temkin models. Kinetic studies show that the pseudo-second-order model best fits the experimental data, indicating that chemisorption is the primary rate-determining process and that the PPOA is a reliable and effective CIP adsorbent. The PPOA demonstrated its usefulness as an environmentally friendly substance for wastewater treatment by performing exceptionally well in simulated wastewater conditions. All things considered, the suggested substance shows a viable method for turning agricultural waste into effective, reusable adsorbents for environmental cleanup.

References

- [1] Z. H. Mussa, A. F. Imran, H. F. S. Al-Saedi, L. R. Al-Ameer, I. F. Deyab, F. F. A-Qaim, and H. Kamyab, "Utilizing pomegranate peel biochar for effective malachite green adsorption," *Results in Surfaces and Interfaces*, vol. 20, pp.100618, 2025. <https://doi.org/10.1016/j.rsurfi.2025.100618>

- [2] H.K. Admawi, and A.A. Mohammed, "A comprehensive review of emulsion liquid membrane for toxic contaminants removal: an overview on emulsion stability and extraction efficiency," *Journal of Environmental Chemical Engineering*, vol. 11, no.3, pp.109936, 2023b. <https://doi.org/10.1016/j.jece.2023.109936>
- [3] J. Fito, K.K. Kefeni, and T.T.I. Nkambule, "The potential of biochar- photocatalytic nanocomposites for removal of organic micropollutants from wastewater," *Science of The Total Environment*, vol. 829, pp.154648, 2022. <https://doi.org/10.1016/j.scitotenv.2022.154648>
- [4] S. A. Abdel Moaty, R. K. Mahmoud, N. A. Mohamed, Y. Gaber, A. A. Farghali, M. S. M. Abdel Wahed, and H. A. Younes, "Synthesis and characterisation of LDH-type anionic nanomaterials for the effective removal of doxycycline from aqueous media," *Water and Environment Journal*, vol. 34, pp. 290-308, 2020. <https://doi.org/10.1111/wej.12526>
- [5] M. S. Fouad, E. F. Mustafa, M. S. Hellal, and M. A. Mwaheb, "A comprehensive assessment of water quality in Fayoum depression, Egypt: identifying contaminants, antibiotic pollution, and adsorption treatability study for remediation," *Scientific Reports*, vol.14, pp.18849, 2024. <https://doi.org/10.1038/s41598-024-68990-8>
- [6] S. M. Bekhit, S. A. Zaki, M. S. El-Din Hassouna, M. Elkadyed, "Effectiveness of fullerene/magnesium oxide nanocomposite in removing ciprofloxacin and tetracycline from aqueous solutions," *RSC Advances*, vol.15, pp. 5190-5201, 2025. <https://doi.org/10.1039/D4RA07938H>
- [7] Z. A. Hammood, and A. A. Mohammed, "Enhanced adsorption of ciprofloxacin from an aqueous solution using a novel CaMgAl-layered double hydroxide/red mud composite," *Results in Engineering*, vol.23, pp.102600, 2024. <https://doi.org/10.1016/j.rineng.2024.102600>
- [8] Y. A. S. Hameed, I.S. S. Alatawi, S. A. Alqarni, A. Ali A. Sari, A. Almahri, A. A. Alfi, N. S. Bedowr, and F. Shaaban, "Effective removal of cefixime using VCu-layered double hydroxide encapsulated with chitosan-carboxymethyl cellulose nanocomposite: Adsorption models and optimization by box-behnken design," *Arabian Journal of Chemistry*, vol.18, no.10, pp.3562025, 2025. https://doi.org/10.25259/AJC_356_2025
- [9] S.B. Zadvarzi, and A.A. Amooey, "Amoxicillin and cefixime simultaneous adsorption by facile synthesized chitosan@polyacrylamide@ZIF-8: Isotherm and kinetic study," *Environmental Sciences Europe*, vol. 35, pp. 60, 2023. <https://doi.org/10.1186/s12302-023-00774-9>
- [10] K. Xu, T. He, L. Li, and X. Xing, F. Jiang, J. Iqbal, P. Han, J. Li, "DTPA-chitosan mushroom waste biochar for efficient removal of tetracycline from wastewater," *Environmental Technology & Innovation*, vol.40, pp. 104472, 2025. <https://doi.org/10.1016/j.eti.2025.104472>
- [11] D. Chang, Y. Mao, W. Qiu, Y. Wu, and B. Cai, "The source and distribution of tetracycline antibiotics in China: a review," *Toxics*, vol. 11, no.3, 2023. <https://doi.org/10.3390/toxics11030214>
- [12] K. Getenew, and A. Misganaw, "Removal of amoxicillin from contaminated water using aloe barbadensis miller bio-adsorbent," *Results in Engineering*, vol. 22, pp.102081, 2024. <https://doi.org/10.1016/j.rineng.2024.102081>
- [13] G. Sulis, S. Sayood and S. Gandra, "Antimicrobial resistance in low- and middle-income countries: current status and future directions," *Expert Review of Anti-infective Therapy*, vol. 20, no. 2, pp. 147–160, 2022. <https://doi.org/10.1080/14787210.2021.1951705>
- [14] N. Kim, B. Cha, Y. Yea, L. K. Njaramba, S. Vigneshwaran, S. S. D. Elanchezhian and C. M. Park, "Effective sequestration of tetracycline and ciprofloxacin from aqueous solutions by Al-based metal organic framework and reduced graphene oxide immobilized alginate biosorbents," *Chemical Engineering Journal*, vol. 450, no. 2, pp.138068, 2022. <https://doi.org/10.1016/j.cej.2022.138068>
- [15] S. Bazgir, S. Farhadi and Y. Mansourpanah, "Adsorptive removal of tetracycline and ciprofloxacin antibiotics from water using magnetic MIL101-Fe metal-organic framework/NiFe₂O₄ decorated with Preysslere-Pope-Jeannin [NaP₅W₃O₁₁]¹⁴⁻ polyanion," *Journal of Solid State Chemistry*, vol. 315, pp. 123513, 2022. <https://doi.org/10.1016/j.jssc.2022.123513>
- [16] S. M. Mahgoub, H. A. Rudayni, A. A. Allam, S. A. Alsalamah, A. Elrafey, R. Abdelazeem, A. A. Kotp, M. M. Abdelsatar, R. Shafie, and R. Mahmoud, "Green removal and waste valorization of ciprofloxacin from water using zinc-iron LDH-chia seed biocomposites: integrated adsorption, computational modeling, and electrochemical conversion," *RSC Advances*, vol.15, pp.37705, 2025. <https://doi.org/10.1039/D5RA06018D>
- [17] A. A. Mohammed, M. A. Atiya, and M. A. Hussein, "Studies on membrane stability and extraction of ciprofloxacin from aqueous solution using pickering emulsion liquid membrane stabilized by magnetic nano-Fe₂O₃," *Colloids and Surfaces A: Physicochemical and Engineering Aspects*, vol. 585, pp. 124044, 2020. <https://doi.org/10.1016/j.colsurfa.2019.124044>

- [18] C. O. Aniagor, C. A. Igwegbe, J. O. Ighalo, and S. N. Oba, "Adsorption of doxycycline from aqueous media: A review," *Journal of Molecular Liquids*, vol. 334, pp.116124, 2021. <https://doi.org/10.1016/j.molliq.2021.116124>
- [19] H.K. Admawi, and A.A. Mohammed, "Extraction of cadmium from aqueous solutions by emulsion liquid membrane (ELM) using three different carriers dissolved in a 70:30 ratio of sunflower oil to kerosene," *Journal of the Indian Chemical Society*, vol.100, pp.101081, 2023a. <https://doi.org/10.1016/j.jics.2023.101081>
- [20] J. Nyirenda, G. Kalaba, and O. Munyati, "Synthesis and characterization of an activated carbon-supported silver-silica nanocomposite for adsorption of heavy metal ions from water," *Results in engineering*, vol.15, pp.100553, 2022. <https://doi.org/10.1016/j.rineng.2022.100553>
- [21] H. K. Admawi, "Adsorption of dye removal from aqueous solutions using natural bitter orange waste: An isotherm and kinetic processes study with efficiency evaluation under optimum conditions," *Progress in Engineering Science*, vol.2, pp.100156, 2025a. <https://doi.org/10.1016/j.pes.2025.100156>
- [22] N. Bellahsen, B. Kakuk, S. Beszédes, Z. Bagi, N. Halyag, T. Gyulavári, S. Kertész, A. El Amarti, E. Tombácz, and C. Hodúr, "Iron-Loaded Pomegranate Peel as a Bio-Adsorbent for Phosphate Removal," *Water*, vol.13, pp.742709, 2021. <https://doi.org/10.3390/w13192709>
- [23] N.H. Solangi, J. Kumar, S.A. Mazari, S. Ahmed, N. Fatima, and N.M. Mujawar, "Development of fruit waste derived bio-adsorbents for wastewater treatment: A review," *Journal of Hazardous Materials*, vol. 416, pp. 125848, 2021. <https://doi.org/10.1016/j.jhazmat.2021.125848>
- [24] N. Hasnaoui, B. Wathelet, and A. Jiménez-Araujo, "Valorization of pomegranate peel from 12 cultivars: dietary fibre composition, antioxidant capacity and functional properties," *Food Chemistry*, vol.160, pp.196–203, 2014. <https://doi.org/10.1016/j.foodchem.2014.03.089>
- [25] A. Hashem, C. O. Aniagor, M. Fikry, G. M. Taha, and S. M. Badawy, "Characterization and adsorption of raw pomegranate peel powder for lead (II) ions removal," *Journal of Material Cycles and Waste Management*, vol.25, pp. 2087–2100, 2023. <https://doi.org/10.1007/s10163-023-01655-2>
- [26] N. A. Hussain, A. Taifi, O. K. A. Alkadir, N. H. Obaid, Z. M. Abboud, A. M. Aljeboree, A. L. Al Bayaa, S. A. Abed, and A. F. Alkaim, "Role of Pomegranate peels as a activated carbon for removal of pollutants," *IOP Conference Series: Earth and Environmental Science*, vol.1029, pp. 012028, 2022. <https://doi.org/10.1088/1755-1315/1029/1/012028>
- [27] M. K. Rashed and W. Tayh, "Removal of Heavy Metals from Wastewater Using Pomegranate Peel," *IOP Conference Series: Materials Science and Engineering*, vol. 881, pp. 012187, 2020. <https://doi.org/10.1088/1757-899X/881/1/012187>
- [28] Ali, S. Afshinb, Y. Poureshgh, A. Azari, Y. Rashtbari, A. Feizizadeh, A. Hamzezadeh, and M. Fazlzadeh, "Green preparation of activated carbon from pomegranate peel coated with zero-valent iron nanoparticles (nZVI) and isotherm and kinetic studies of amoxicillin removal in water," *Environmental Science and Pollution Research*, vol.27, pp. 36732–36743, 2020. <https://doi.org/10.1007/s11356-020-09310-1>
- [29] O. J. Al-sareji, M. Meiczinger, R. A. Al-Juboori, R. A. Grmasha, M. Andredaki, V. Somogyi, I. A. Idowu, C. Stenger-Kovács, M. Jakab, E. Lengyel, K. S. Hashim, "Efficient removal of pharmaceutical contaminants from water and wastewater using immobilized laccase on activated carbon derived from pomegranate peels," *Scientific Reports*, vol.13, pp.11933, 2023. <https://doi.org/10.1038/s41598-023-38821-3>
- [30] S. A. Hassan, and F. J. Ali, "Equilibrium, thermodynamics, and kinetics study of doxycycline adsorption from aqueous solution using spent black tea leaves and pomegranate peel wastes", *International Journal of Development Research*, vol. 4, pp. 129-135, 2014.
- [31] F. Al-Badaii, K. M. Jansar, N. A. Ab Jalil, A. Abdul Halim, "Sustainable boron removal from aqueous solutions using pomegranate peel adsorbents: A comprehensive study on isotherms, kinetics, and thermodynamics," *Desalination and Water Treatment*, vol.317, pp. 100045, 2024. <https://doi.org/10.1016/j.dwt.2024.100045>
- [32] R. Rai, R. L. Aryal, H. Paudyal, S. K. Gautam, K. N. Ghimire, M. R. Pokhrel, and B. R. Poudel, "Acid-treated pomegranate peel; An efficient biosorbent for the excision of hexavalent chromium from wastewater," *Heliyon*, vol. 9, pp. e15698, 2023. <https://doi.org/10.1016/j.heliyon.2023.e15698>
- [33] C. Waghmare, S. Ghodmare, K. Ansari, F. M. Alfaisal, S. Alam, M. A. Khan, Y. Ezaier, "Adsorption of methylene blue dye onto phosphoric acid-treated pomegranate peel adsorbent: Kinetic and thermodynamic studies," *Desalination and Water Treatment*, vol. 318, pp. 100406, 2024. <https://doi.org/10.1016/j.dwt.2024.100406>
- [34] M. A. Ahmad, and R. Alrozi, "Optimization of rambutan peel based activated carbon preparation conditions for Remazol Brilliant Blue R removal," *Chemical Engineering Journal*, vol.168, pp. 280–285, 2011. <https://doi.org/10.1016/j.cej.2011.01.005>
- [35] H.K. Admawi, and A.A. Mohammed, "Nano Green emulsion liquid membrane for the simultaneous extraction of heavy metals from real wastewater," *Discover Chemistry*, vol. 2, pp.74, 2025b. <https://doi.org/10.1007/s44371-025-00149-4>
- [36] S. Shewatatek, and G. Gonfa, "Sintayehu Mekuria Hailegiorgis, Belete Tessema, Adsorptive removal of Cr (VI) from aqueous solution using sulfuric acid-treated diatomite," *Results in Chemistry*, vol. 15, pp.102205, 2025. <https://doi.org/10.1016/j.rechem.2025.102205>

- [37] M. Alishiri, S. A. Abdollahi, A. N. Neysari, S. F. Ranjbar, N. Abdoli, and M. Afsharjahanshahi, "Removal of ciprofloxacin and cephalexin antibiotics in water environment by magnetic graphene oxide nanocomposites; optimization using response surface methodology," *Results in Engineering*, vol. 20, pp. 101507, 2023. <https://doi.org/10.1016/j.rineng.2023.101507>
- [38] R. Foroutan, S. J. Peighambaroudost, S. Hemmati, A. Ahmadi, E. Falletta, D. B. Ramavandi, C. L. Bianchi, "Zn²⁺ removal from the aqueous environment using a polydopamine/hydroxyapatite/Fe₃O₄ magnetic composite under ultrasonic waves," *RSC Advances*, vol.11 pp.27309, 2021. <https://doi.org/10.1039/D1RA04583K>
- [39] S.I.S. Al-Hawary, A. Khodadadi, S. Shahab, S.J. Saadoun, N. Mengelizadeh, D. Balarak, and K.A.M. Al-Zaidy, "Photocatalytic degradation of acid blue 113 dye by Montmorillonite/Copper ferrite nanocomposite: characterization, optimization, and toxicity assessment," *Chemical Physics Impact*, vol.10, pp.100857, 2025. <https://doi.org/10.1016/j.chphi.2025.100857>
- [40] Y. Yahia, K. T. Rashid, Razak, M. A. Shehab, M.Y. Ghadhban, A. A. Abdul Munaf Al-lami, M. A. T. Al Mayyahi, M. A. Salih, H. H. Mohammed, and A. Mahmood, "Treating wastewater contaminated with congo red (CR) dye using an optimized polyethersulfone/ propolis (bee glue) PES/PRS ultrafiltration membrane," *RSC Advances*, vol.15, pp.23174, 2025. <https://doi.org/10.1039/D5RA03565A>
- [41] A.I. Alwared, T.J. Al-Musawi, L.F. Muhain, and A.A. Mohammed, "The biosorption of reactive red dye onto Orange peel waste: a study on the isotherm and kinetic processes and sensitivity analysis using the artificial neural network approach," *Environmental Science and Pollution Research*, vol.28, pp. 2848–2859, 2021. <https://doi.org/10.1007/s11356-020-10613-6>
- [42] H. Bousemat, S. Ziane-Hezil, B. S. Hadjer, F. Bessaha, G. Bessaha, A. Çoruh, M. Sillanpää, and M. A. Khan, "Experimental and modeling studies for the simultaneous removal anionic dyes in single and binary systems using activated clay," *Scientific Reports*, 2025. <https://doi.org/10.1038/s41598-025-30039-9>
- [43] N.S. Ali, N.M. Jabbar, S.M. Alardhi, H.S. Majdi, and T.M. Albayati, "Adsorption of methyl violet dye onto a prepared bio-adsorbent from date seeds: isotherm, kinetics, and thermodynamic studies," *Heliyon*, vol.8, pp. e10276, 2022. <https://doi.org/10.1016/j.heliyon.2022.e10276>
- [44] I.O. Saheed, W.D. Oh, and F.B.M. Suah, "Chitosan modifications for adsorption of pollutants - a review," *Journal of Hazardous Materials*, vol.408, pp.124889, 2021. <https://doi.org/10.1016/j.jhazmat.2020.124889>
- [45] M. Shirmardi, A.H. Mahvi, A. Mesdaghinia, S. Nasser, and R. Nabizadeh, "Adsorption of acid red18 dye from aqueous solution using single-wall carbon nanotubes: kinetic and equilibrium," *Desalination and Water Treatment*, vol. 51, pp.6507–6516, 2013. <https://doi.org/10.1080/19443994.2013.793915>
- [46] G. Zhu, J. Wang, X. Zhao, S. Zhang, C. Wei, C. Liu, L. Cao, S. Zhao, J. Zhang, and S. Zhang, "Effective removal of tetracycline antibiotics from water by in-situ nitrogen-doped porous biochar derived from waste antibiotic fermentation residues," *Journal of Environmental Chemical Engineering*, vol.12 (6), pp.114433, 2024. <https://doi.org/10.1016/j.jece.2024.114433>
- [47] Z. Liu, K. Huang, Y. Zhang, D. Tian, M. Huang, J. He, J. Zou, L. Zhao, F. Shen, "Biochar produced by combining lignocellulosic feedstock and mushroom reduces its heterogeneity," *Bioresource Technology*, vol.355, pp. 127231, 2022. <https://doi.org/10.1016/j.biortech.2022.127231>
- [48] Z. Shao, Shuangbao, S. Wu, Y. Gao, X. Liu, and Y. Dai, "Two-step pyrolytic preparation of biochar for the adsorption study of tetracycline in water," *Environmental Research*, vol. 242, pp. 117566, 2024. <https://doi.org/10.1016/j.envres.2023.117566>
- [49] A.A. Mohammed, and Z.A. Hammood, "Efficient removal of sulfamethoxazole antibiotic from aqueous solution using red mud/layered double hydroxide nanocomposite: optimization, kinetic, and isotherm studies," *Results in Surfaces and Interfaces*, vol.19, pp.100534, 2025. <https://doi.org/10.1016/j.rsufi.2025.100534>
- [50] M. T. Rahman, F. B. Sagar, M. L. Rahman, F. Rahman, M. M. R. Nahid, and N. Sharmin, "Efficient adsorptive removal of ciprofloxacin from wastewater using alginate bearing Mg–Al layered double hydroxide," *Journal of the Indian Chemical Society*, vol.102, pp.101519, 2025. <https://doi.org/10.1016/j.jics.2024.101519>
- [51] N. Dhiman, and N. Sharma, "Batch adsorption studies on the removal of ciprofloxacin hydrochloride from aqueous solution using ZnO nanoparticles and groundnut (*Arachis hypogaea*) shell powder: a comparison," *Indian Chemical Engineer*, vol. 61, pp. 67-76, 2019. <https://doi.org/10.1080/00194506.2018.1424044>

امتزاز السيبروفلوكساسين على مادة ماصة من قشر الرمان المعالج بحمض الأوليك: دراسات متساوية الحرارة، وحركية، وديناميكية حرارية، وإحصائية

حيدر كامل عظاموي^{١*}

^١ قسم التخطيط البيئي، كلية التخطيط العمراني، جامعة الكوفة، النجف، العراق

الخلاصة

تمت دراسة أداء المادة المازة المصنوعة من قشور الرمان المعالجة بحمض الأوليك (PPOA) باستخدام طريقة الدفعات (Batch method) لامتزاز السيبروفلوكساسين (CIP) من محلول مائي. على الرغم من أن دراسات أخرى قد بحثت في التحسين الكيميائي للمواد المازة باستخدام عوامل كيميائية مختلفة، إلا أن الاستخدام المبتكر لحمض الأوليك في التحسين يُحقق نتائج غير مسبوقة من حيث كفاءة إزالة السيبروفلوكساسين. تم تحسين الإزالة من خلال دراسة درجة حموضة العينة، وفترة التلامس، والتركيز الأولي للسيبروفلوكساسين، وجرعة المادة الماصة باستخدام منهجية سطح الاستجابة (RSM) مع تصميم مركزي مركب (CCD)، حققت جرعة ٠,٣ غ/١٠٠ مل كفاءة إزالة ممتازة (أكثر من ٨١%) لتركيزات السيبروفلوكساسين البالغة ٦٠ ملغ/لتر بعد ٩٠ دقيقة من التلامس عند درجة حموضة ٦. بمعامل ارتباط (R^2) مقداره ٠,٩٨٥، أظهر تحليل التباين (ANOVA) القائم على تصميم CCD-RSM تطابقاً جيداً بين النتائج التجريبية وتوقعات النموذج التربيعي. وُجد أن نموذج لانغموير الحراري يُطابق منحنيات امتزاز السيبروفلوكساسين (CIP) على قشر الرمان (PPOA) بدقة عالية، حيث بلغت قيمة الامتزاز القصوى النظرية ١٩,٩٠ ملغم/غم، مما يشير إلى امتزاز أحادي الطبقة. علاوة على ذلك، يُمكن لنموذج التفاعل من الرتبة الثانية (The pseudo-second-order model) وصف حركية الامتزاز بدقة، مما يُشير إلى تأثير معدل الامتزاز بالامتزاز الكيميائي. تتمثل الآليات الرئيسية لامتناس السيبروفلوكساسين الحيوي في التبادل الأيوني والتجاذب الكهروستاتيكي، بينما تخضع آليات الامتزاز لانتقال الكتلة الخارجي وانتشار جزيئات السيبروفلوكساسين على سطح المادة المازة وداخل فجواتها. أكد التحليل الديناميكي الحراري أن الامتزاز كان طارداً للحرارة وتلقائياً. بعد أربع دورات متتالية على ذات المادة المازة، انخفضت كفاءة إمتزاز المادة المازة من ٨١,٨٨% إلى ٥٠,٩١%، مما يدل على إمكانية إعادة استخدامها. أظهرت النتائج أن قشر الرمان مادة مازة صديقة للبيئة وغير مكلفة لإزالة السيبروفلوكساسين. وباستخدام هذا المنتج الثانوي للمخلفات الزراعية، تمت إزالة السيبروفلوكساسين بفعالية.

الكلمات الدالة: سيبروفلوكساسين، حمض الأوليك، الامتزاز، قشور الرمان، معالجة مياه الصرف الصحي.